Third Chinese-German Joint Symposium on Coastal and Ocean Engineering
National Cheng Kung University, Tainan
November 8-16, 2006

A multi-decadal medium-resolution wind, wave and storm surge hindcast suitable for coastal applications

Ralf Weisse Hans von Storch Heinz Günther Frauke Feser
Institute for Coastal Research
GKSS Research Centre, Geesthacht
weisse@gkss.de storch@gkss.de guenther@gkss.de feser@gkss.de

Andreas Plüß
Federal Waterways Research and Engineering Institute
Coastal Division, Hamburg
pluess@hamburg.baw.de

Abstract

A multi-decadal medium-resolution met-ocean hindcast for the North Sea and parts of the Northeast Atlantic is presented. The hindcast is based on a dynamical downscaling of the global NCEP/NCAR weather re-analyses using some simple data assimilation techniques. It is shown that the reconstructed wind, wave and storm surge climate agree reasonably with available in-situ observations. Analysis of the wind, wave and storm surge climate based on hindcast data reveals that they have undergone considerable variations from year to year and on longer time scales. An increase in storm activity from the beginning of the hindcast period has levelled off later and was replaced by a downward trend over the northeast North Atlantic. This behaviour closely corresponds to that based on the analysis of proxies for storm activity. Changes in extreme wave and storm surge conditions show a similar pattern over much of the North Sea area.

1 Introduction

A multi-decadal (1948-2006) medium-resolution wind, wave and storm surge hindcast for the North Sea is presented. The hindcast is based on the National Centers for Environmental Prediction (NCEP) reanalysis for the same period. While this reanalysis presently represents one of the longest, most comprehensive, and most homogeneous weather data sets, it neither contains information on wind waves or storm surges nor is its spatial (about 210 km x 210 km) or temporal (6 hours) resolution adequate for coastal applications. Partly within the European project HIPOCAS (Hindcast of Dynamic Processes of the Ocean and the Coastal Areas of Europe) the NCEP reanalysis has therefore been

utilized to first drive a regional atmosphere model at sufficiently high resolution for regional scales. Subsequently, wind and pressure fields from this simulation have been used to run regional storm surge and wind wave models. This way, consistent met-ocean data sets for the past 59 years have been reconstructed. Here results of this effort for the North Sea are presented. The data set comprises wind, surface pressure and other atmospheric variables as well as two-dimensional ocean wave spectra, water levels and currents every hour for the period 1948-2006. The spatial resolution varies between about
50 km x 50 km for atmospheric variables, about 5 km x 5 km for ocean waves and about 100 m for water levels and currents near the coast. It is demonstrated that this consistent met-ocean reconstruction reasonably describes the statistics of the observed met-ocean conditions of the recent past and is suitable for coastal applications, either directly or as boundary conditions for subsequent high-resolution coastal models. This way this data set may complement the analysis of existing observations, for instance when the parameters of interest have either not been observed directly, or have been sampled only at insufficient spatial and temporal detail. We will present the approach for the HIPOCAS (Soares et al. 2002) hindcast. Results for the North Sea will be compared with observations and it will be demonstrated that reasonable descriptions of the extreme value statistics may be inferred. Multi-decadal trends and variations in the storm climate and their relation with ocean wave and storm surge conditions are discussed.

2 The 1948-2006 met-ocean hindcast

A consistent met-ocean hindcast for the period 1948-2006 was performed. The hindcast consists of a dynamical downscaling of the NCEP/NCAR global weather re-analyses (Kalnay et al. 1996; Kistler et al. 2001) using a regional atmosphere model for the North Sea and the Northeast Atlantic in combination with a simple data assimilation approach (Feser et al. 2001; von Storch et al. 2000). From this experiment hourly wind fields have subsequently been used to run high-resolution storm surge (Weisse and Plüß 2006) and wave model hindcasts for the North Sea (Weisse and Günther 2006). Figure 1 shows the principal set-up of the met-ocean hindcast. In the following, some information about the technical details is provided.

2-1 The atmosphere hindcast

The hindcast was performed using the atmosphere model REMO (Jacob and Podzun 1997) and is described in detail in Feser et al. (2001). The purpose of this integration was to provide a reconstruction of the regional atmospheric conditions during 1948–2006 for Europe and adjacent seas. In this integration, the model was forced by the NCEP/NCAR reanalysis. The NCEP/NCAR forcing was provided at eight grid points at the lateral boundaries using the classical approach described by Davies (1976). Additionally, the

NCEP/NCAR large-scale circulation was forced upon the regional model using the

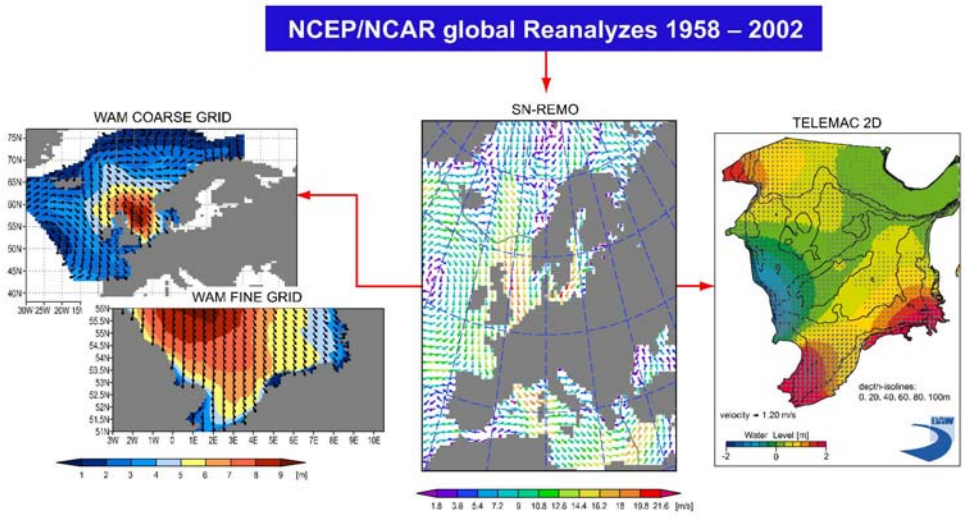

Figure 1: Layout of the consistent met-ocean hindcast 1948-2006 for the Southern North Sea. From the regional atmosphere hindcast (middle) hourly wind fields were used to force a tide-surge (right) and a wave model hindcast (left). The figure shows an example of consistent met-ocean conditions obtained from the hindcast for 12 UTC on 21 February 1993. Middle: near-surface (10 m height) marine wind fields in ms^{-1} and corresponding wind direction obtained from the regional atmospheric reconstruction. Left: corresponding significant wave height fields in m and mean wave direction from the coarse and the fine grid wave model hindcast. Right: Tide-surge levels in m from the corresponding tide-surge hindcast (after Weisse and Günther 2006).

spectral nudging approach suggested by von Storch et al. (2000). Spectral nudging may be seen as a suboptimal and indirect data assimilation technique (von Storch et al. 2000), depending on the quality of the global forcing fields. In case no further observations are available for assimilation into the regional model, spectral nudging can be considered as a simple approach to “assimilate” those scales of the global reanalysis in which we have the highest confidence. In other words, we would not like the regional model to *significantly* modify those scales that are reasonably resolved by the global reanalysis and that are supported by data assimilation. Weisse and Feser (2003) showed that the representation of extreme events in near-surface wind speed could indeed be improved in a regional atmosphere model simulation when the spectral nudging approach was adopted. In the following, we will refer to a REMO setup utilizing the spectral nudging approach as SN-REMO. The SN-REMO hindcast has been performed on an about 50 km x 50 km grid covering Europe, the Baltic Sea, the North Sea, and adjacent parts of the northeast North Atlantic. Full model output including near-surface wind speed and direction has been stored every hour.

2-2 The storm surge hindcast

The hindcast was performed using the TELEMAC2D code from Electricité de France (EDF) (Hervouet and Haren 1996) and is described in detail in Weisse and Plüß (2006).

The model applies time and space variable wind fields obtained from the above mentioned atmospheric hindcast to account for the external forces at the interface between water and air. The complex coastline, islands, and bathymetric structures in the coastal zone and the mouths of the estuaries coupled with the whole North Sea region demand for the use of an unstructured mesh (triangles). The calculation mesh consists of approximately 50,000 triangular elements and 27,000 nodes the distance of which varies between about 75 m near the coast and in the estuaries and 27 km in open sea regions. The dimension of the hydrodynamic model domain is shown in Figure 1. For details see Plüß (2004). Lateral boundary conditions, time series of the water levels, were calculated by reanalyzing the tidal harmonic constants for each boundary location. This procedure includes the variation of the tidal amplitudes due to the variation of the nodal tidal cycle. The prediction of the steering forces at the lateral boundaries using the harmonic tide analysis of the tidal constants lacks of longer periodic/aperiodic water level changes. These effects are known as external surges. To enhance the model results, filtered surge levels at Aberdeen have been assimilated into the model. The methodology and the impact on the model results are described in Weisse and Plüß (2006). From the tide-surge model simulation water levels and barotropic velocity components have been stored every hour for all grid points.

2-3 The wave model hindcast

For the wave hindcast the wave model WAM (WAMDI Group 1988) was set-up in a nested version with a coarse grid covering the entire North Sea and large parts of the northeast North Atlantic and a fine grid covering the North Sea south of 56 S (Southern North Sea). The spatial resolutions were about 50 × 50 km and 5.5 × 5.5 km for the coarse and the fine grid respectively. For both grids wave spectra were computed with a directional discretisation of 15 degrees and at 28 frequencies ranging non-linearly from about 0.042 Hz to 0.55 Hz. The latter corresponds to wave lengths between about 5 m and 900 m. For the fine grid, the wave model was run in shallow water mode while for the coarse grid observed sea ice conditions from the Norwegian Meteorological Institute have been taken into account. The wave model has been driven by hourly wind fields derived from the above mentioned atmosphere hindcast. For the fine grid wave model simulation two-dimensional wave spectra have been stored every 3 hours, while integrated wave parameters such as significant wave height, mean wave direction and different wave periods are available every hour.

3 Results

3-1 Model Validation

Figure 2 shows a comparison between observed and hindcast wind speed and direction as well as significant wave height, period and wave direction for a three months period at station K13 (53.22 N, 3.22 E). In principal a good agreement can be inferred. For instance, the storm event on 21 February which caused observed significant wave heights of more than 6 m is reasonably reproduced for all parameters. On the other hand, there are also events with larger discrepancies such as the one around 1 March for which wave heights are considerably underestimated, in this case caused by too low wind speeds in the atmospheric hindcast (Figure 2).

A comparison for the entire period for which observations were available at K13 is presented in Figure 3. For wind speed very little bias can be inferred and the frequencies with which severe events are over- or underestimated are essentially the same. The latter indicates that while individual storms may or may not be captured by the hindcast their statistics remain unbiased and the hindcast may be used as substitute reality to study the statistics of extreme events and their long-term variability. A similar conclusion holds for wind direction and significant wave height while some tendency to overestimate the most extreme wave periods can be inferred. A similar comparison was made for some more stations (see Weisse and Günther 2006).

To investigate in particular the extent to which extreme value statistics are reproduced we analyzed and compared return values derived from hindcast and observed data (Table 1). For wind speed the estimated return periods agree well within the 90%-confidence limit estimated from Monte Carlo simulations. A similar conclusion holds for the significant wave height at K13 and EUR although hindcast return periods systematically appear to be above the observed ones. For SON surrounded by rather shallow water, hindcast return periods are significantly different from the observed ones with the hindcast overestimating observations. The latter may be partially explained by the 5.5 km × 5.5 km resolution of the wave model in which the shoals surrounding SON are not very well resolved.

Figure 4 shows a comparison between observed and hindcast water levels for Borkum and Cuxhaven. For both stations, the comparison was made between hourly data. Because of the limited data available, the comparison for Borkum is restricted to the period 1985–2002, while for Cuxhaven the period 1958–2002 is considered. A good agreement between observed and hindcast water levels is obtained at both locations in general. There is a tendency to overestimate the lowest water levels at both stations while no such tendency can be inferred for the highest water levels. In particular for high waters,

the

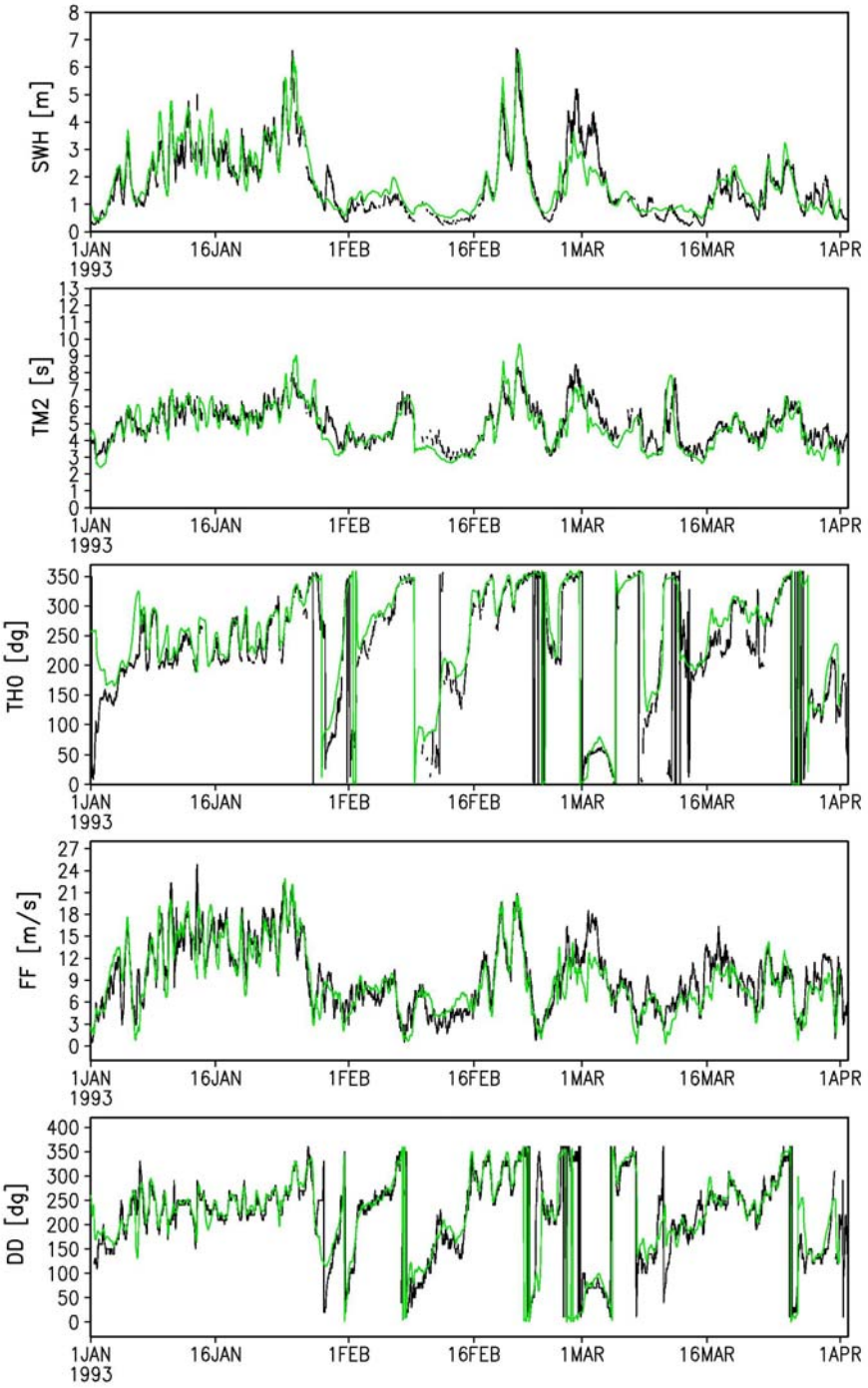

Figure 2: Time series of significant wave height in m, Tm2 wave period in s, mean wave direction in degrees coming from, wind speed in ms^{-1} and wind direction in degrees coming from (from top to bottom) at K13 for a three months period 01 January 1993-31 March 1993. Observations - black, model results – green (after Weisse and Günther 2006).

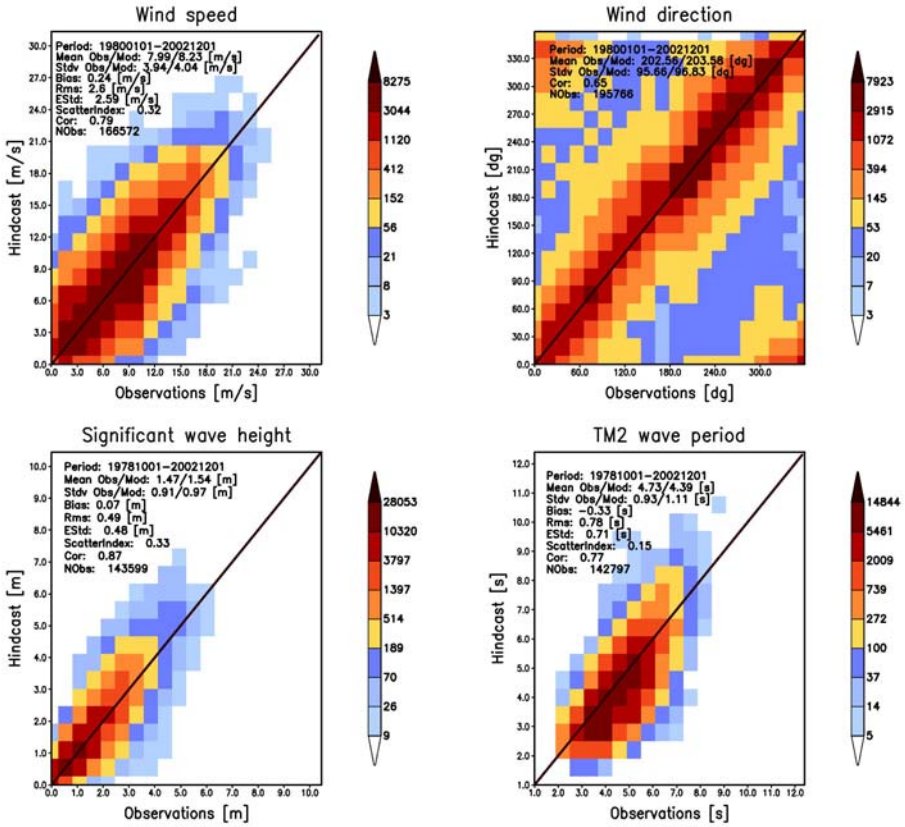

Figure 3: Scatterplot between observed (x-axis) and hindcast (y-axis) hourly wind speeds in ms^{-1} (upper left), wind direction in degrees coming from (upper right), significant wave height in m (lower left) and Tm2 wave period in s (lower right) at K13. Colours indicate the numbers of cases in each class. In addition the following statistics are presented (from top): Analysis period, observation and hindcast mean, observation and hindcast standard deviation, bias and root-mean-square error between observations and hindcast, standard deviation of the differences between hindcast and observations, scatter index, correlation and number of observed/hindcast data values that have been used in the analysis (after Weisse and Günther 2006).

		Wind [m/s]						**Waves [m]**					
		Hipocas			***Observed***			***Hipocas***			***Observed***		
	Years	x_r^{90}	x_r	x_r^{90}	x_r^{90}	x_r	x_r^{90}	x_r^{90}	x_r	x_r^{90}	x_r^{90}	x_r	x_r^{90}
K13	**2**	24.38	25.17	25.96	24.05	25.21	26.37	7.12	7.49	7.86	6.41	6.77	7.13
	5	25.86	27.28	28.70	25.75	27.64	29.53	7.84	8.44	9.04	6.93	7.54	8.15
	25	28.44	31.33	34.22	28.09	32.77	37.45	8.99	10.35	11.71	7.52	9.21	10.90
EUR	**2**	22.50	23.16	23.82	23.16	24.03	24.90	5.89	6.15	6.41	5.52	5.84	6.16
	5	23.76	24.82	25.88	24.33	25.94	27.55	6.34	6.83	7.32	5.89	6.46	7.03
	25	25.67	28.00	30.33	26.43	29.75	33.07	6.90	8.20	9.50	5.99	7.88	9.77
SON	**2**	23.29	24.15	25.01	23.11	24.03	24.95	6.78	7.06	7.34	5.60	5.84	6.08
	5	24.89	26.32	27.75	24.15	25.94	27.73	7.37	7.79	8.21	5.97	6.46	6.95
	25	26.68	30.70	34.72	26.42	29.75	33.08	8.04	9.03	10.02	6.34	7.88	9.42

Table 1: Comparison of 2, 5, and 25-year return values x_r estimated from observed and hindcast wind speed and significant wave height at K13, Europlatform (EUR), Huibertgat (HBG) and Schiermonnikoog (SON). Additionally shown is the 90% confidence interval x^{90}_r obtained from 1000 Monte Carlo simulations each. *T* denotes the return periods (after Weisse and Günther 2006).

hindcast appears to be calibrated, i.e., there is no systematic bias between observations and model values, and the probabilities for the hindcast to over- or underestimate observed water levels appear to be similar. Long-term root-mean-square-errors are smaller than 30 cm and the correlation between observed and hindcast hourly water levels is above 0.95 for both stations.

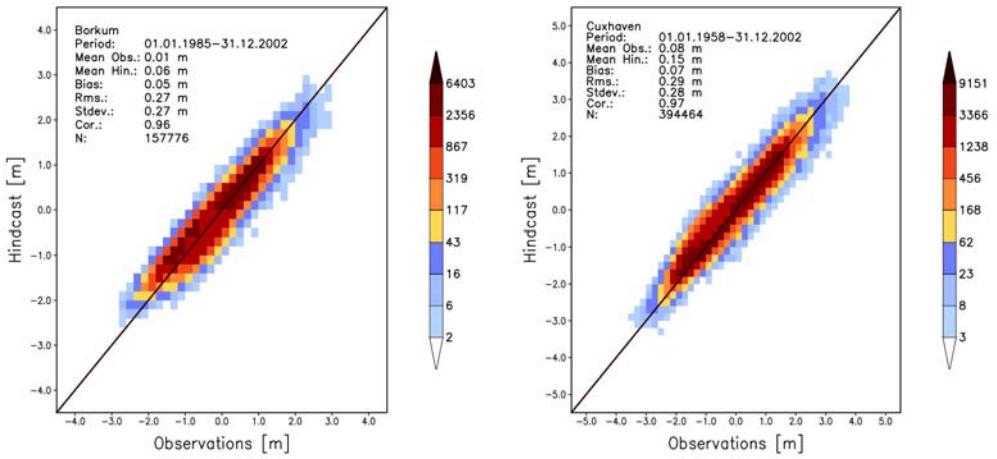

Figure 4: Scatterplot between observed (x-axis) and hindcast (y-axis) hourly water levels at Borkum (left) and Cuxhaven (right). Colours indicate the number of cases in each 0.2 m×0.2 m box. In addition, the following statistics are presented (from top): analysis period, observation mean, hindcast mean, bias and root-mean-square error between observations and hindcast, standard deviation of the differences between hindcast and observations, correlation, and number of observed/hindcast data values that have been used in the analysis (after Weisse and Plüß 2006).

A similar plot for the storm surge component of the water level fluctuations has been provided by Weisse and Plüß (2006). They showed that for Cuxhaven, there is again a small tendency to overestimate the lowest surges. The largest surges appear to be reasonably simulated at both stations. Root-mean-square errors between observed and hindcast storm surges are in the order of about 15 cm and the correlations are 0.92 for both stations. A rather good agreement between observed and modelled values can again be inferred in general. The model also reasonably simulates the observed inter-annual variations. This was demonstrated by Weisse and Plüß (2006) by a comparison between observed and hindcast annual winter mean and winter 90-percentile high waters.

In summary, we conclude that the multi-decadal met-ocean hindcast reasonably simulates the observed conditions, both on short and long (year to year) time scales. Some more details on model validation can be found in Weisse et al. (2005) and Koch and Feser (2006) for wind fields, in Weisse and Plüß (2006) for water levels and in Weisse and Günther (2006) for sea states.

3-2 Hindcast wind, wave and storm surge climate

Weisse et al. (2005) analyzed the long-term average number of storms in the regional atmosphere model hindcast. Within the model domain, they found the highest storminess being associated with the exit of the North Atlantic storm track with a maximum located approximately south of Iceland (their Figure 4). Here, on average, more than 50 storms per year with wind speeds exceeding Beaufort 7 do occur. From these storms, approximately 12%–14% are classified as severe storms having wind speeds of more than 10 Beaufort. The remainder represents moderate storms with maximum wind speeds between 8 and 10 Beaufort. Over the North Sea, on average, only one or two severe storms are found per year. South of about 45°N no severe storms were identified in the simulation.

Weisse and Günther (2006) analyzed the long-term wave climate in the wave model hindcast. They concentrated on the local long-term (1958-2002) 99%-ile of total significant wave height as a threshold to determine severe wave conditions. For hourly values this threshold, on average, is exceeded for 3-4 days a year. Based on this severe event threshold (SET) they defined several parameters describing the characteristics of severe wave event statistics such as the annual number of events exceeding the SET, their average duration or intensity. The long-term averages of these parameters for the Southern North Sea are shown in Figure 5. It can be inferred that the 99%-ile significant wave height (SET) is generally largest towards the North of the model domain where it reaches values of up 6.5 m. Towards the South and towards the coasts the long-term 99%-ile wave height generally decreases reaching values of about 4-5 m in the German Bight and off the coasts. For large parts of the Southern North Sea typical values of about 5-6 m are found. For most parts of the Southern North Sea the severe event threshold is exceeded on average 8-9 times a year. An exception is provided by parts of the UK coast where extreme events occur a little less frequent. Once the significant wave height is above the SET, it remains there on average for about 10-11 hours for large parts of the Southern North Sea. Again, an exception is found for the UK coast where the duration of the events is somewhat longer. Typical intensities of the events vary between about 0.8-1.3 m above the SET. For each event exceeding the local SET Weisse and Günther (2006) determined a characteristic Tm2-period and mean wave direction. Considering all extreme events 1958-2002 they found that severe waves in the Southern North Sea typically have periods of about 8-9 s. Off the UK coasts periods typically range from 7-8 s while even smaller periods are found close to the English Channel. In the eastern part severe wave events most frequently approach from westerly to north-westerly directions. In the western part severe events more typically arrive from north-westerly or northerly directions. Along a small stripe at the UK coast severe wave events are usually approaching from easterly directions. This behaviour can be associated with the typical eastward path of mid-latitude cyclones and the sheltering effect of the UK land mass.

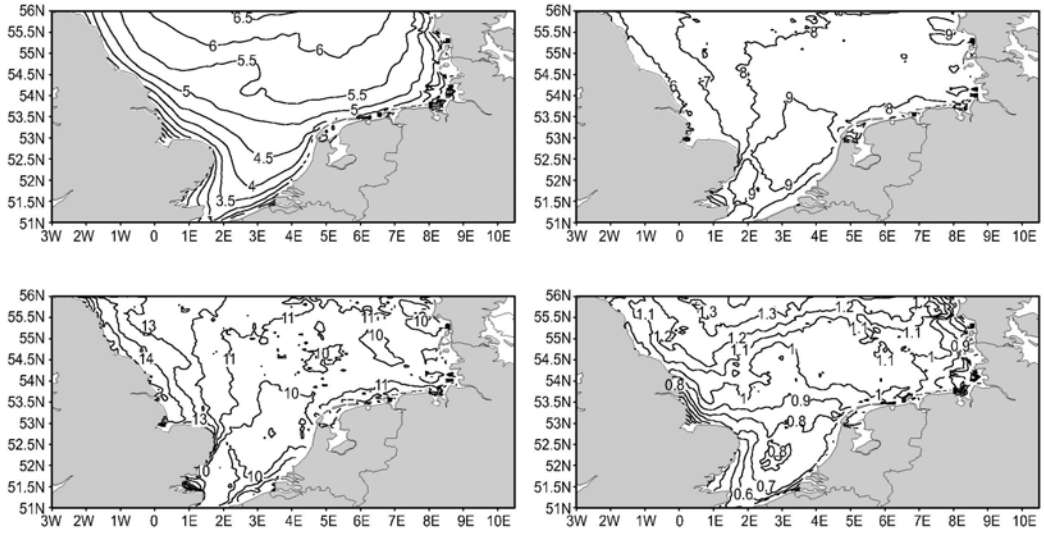

Figure 5: Long-term 1958-2002 99%-ile of total significant wave height in m (SET, upper left), the average number of events per year exceeding the SET (upper right), the average duration in h (lower left) and the average intensity in m (lower right) of these events (after Weisse and Günther 2006).

The climate of the storm-surge hindcast is described in Weisse and Plüß (2006). They analyzed long-term average storm surges along a cross-section following the North Sea coast line from the UK to Denmark. They generally found highest surges along the coastlines in the German Bight with pronounced year-to-year variability superimposed.

3-3 Long-term changes in wind, wave and storm surge climate

Long-term changes in the wind, wave and storm surge climate of the met-ocean hindcast are described in detail Weisse et al. (2005), Weisse and Plüß (2006) and Weisse and Günther (2006). For the storm climate they showed that it has undergone significant variations on time scales from year-to-year and longer. In particular an increase in the northeast North Atlantic north of about 40 N from about 1958-1990/1995 is noted. This increase has levelled off afterwards in the North Sea and was replaced by a downward trend over the Northeast Atlantic. This behaviour is in agreement with the analysis of storm activity based on proxy data (Alexandersson et al. 1998, 2000). The latter reveal that in the area storm activity was rather weak around 1960. After that it increased until about 1990/1995. After 1995 storm activity decreased and the levels of activity found around 1990-1995 are comparable to that observed at the beginning of the 20th century (Alexandersson et al. 2000).

The long-term changes of waves and storm surges in the met-ocean hindcast closely correspond to those described for storm activity. An example for severe wave event characteristics in the German Bight is provided in Figure 6. Here extreme wave heights have

increased from the beginning of the simulation period until a maximum (in the running mean time series) between about 1990 and 1995 is reached. Afterwards a decrease in extreme wave heights seems to prevail. This long-term development can be decomposed into an increase of the frequency of severe wave events that has levelled off around 1985 and an attenuation in the intensity and the duration of these events (Figure 6) although more data after 2002 are needed to fully assess the significance in the change of the extreme wave height trends. However, as the development for the number of severe wave events closely corresponds to that reported for the number of storms in the area (Weisse et al. 2005) and the evolution of the annual wave height 99%-iles parallels that described for percentile based North Sea storm indices derived from pressure observations (Alexandersson et al. 2000) it may remain likely that the attenuation of severe wave events has continued until now as an update of the storm indices reveals decreasing storm activities until 2005 (von Storch, pers. comm. 2005). For the UK coast and the South-western North Sea somewhat different patterns are obtained: While there is hardly any noticeable change except for a slight and non-significant decreasing trend along the UK coast, for the southwestern North Sea an increase in extreme wave conditions is found that is most pronounced at the beginning of the hindcast period and which has levelled off later (not shown).

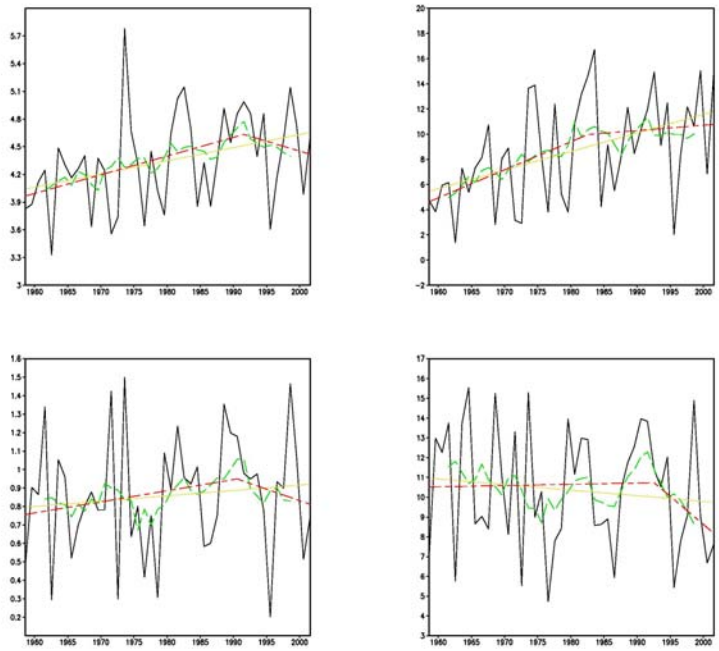

Figure 6: Inner German Bight: Time series of annual 99%-iles of significant wave height in m (upper left), annual number of events exceeding the SET (upper right), their average intensity in m (lower left) and their average duration in h (lower right). Time series from annual values (black), 7-yr running means (green), linear trend (yellow) and piecewise linear trends (red) (after Weisse and Günther 2006).

4 Summary and discussion

A multi-decadal medium-resolution met-ocean hindcast for the North Sea and parts of the Northeast Atlantic was presented. The hindcast is based on a dynamical downscaling of the global NCEP/NCAR weather re-analyses using some simple data assimilation techniques. It was shown that the reconstructed wind, wave and storm surge climate agrees reasonably with available in-situ observations. Analysis of long-term changes reveals that the storm activity has increased from the beginning of the hindcast period over much of the model domain. The increase has levelled off later and has been replaced by a downward trend around 1990/1995 over parts of the northeast North Atlantic. This behaviour corresponds to that obtained from an analysis of proxy data for storminess. The latter shows pronounced decadal variability with relatively high storm activity around 1990/1995 and at the beginning of the 20th century, while storm activity was low around about the 1960s and a decrease after 1990/1995 is observed (Alexandersson et al. 2000). A similar and consistent behaviour was found from the analysis of the hindcast wave and storm surge conditions.

Data from the met-ocean hindcast are available every hour for the hindcast period 1948-2006 and at rather high spatial resolution ranging from about 50 km for the atmosphere hindcast to about 75 m for the oceanic reconstruction close to the North Sea coast line. While there are some limitations of the applicability of the hindcast data such as for the analysis of extreme wave heights in rather shallow water, Gaslikova and Weisse (2006) showed that the hindcast data provide a reasonable source for boundary conditions for very high-resolution modelling with shallow water wave models in coastal environments. Apart from the direct analysis of long-term variability and changes the hindcast may be a valuable source of information for a large variety of applications. In particular when sufficiently long, homogeneous and consistent observational met-ocean data do not exist the hindcast may be used as a reality substitute complementing the analysis of the limited observational material available. Such applications may include for instance analyses needed for coastal protection, offshore wind farms, shipping and navigation or ocean transports. Some examples can be found at the coastDat portal (www.coastdat.de).

5 References

Alexandersson, H., T. Schmith, K. Iden, and H. Tuomenvirta, 1998. Long-term variations of the storm climate over NW Europe, *Global Atmos. Oc. System*, Vol. 6, pp 97-120.

Alexandersson, H., H. Tuomenvirta, T. Schmidth, and K. Iden, 2000. Trends of storms in NW Europe derived from an updated pressure data set, *Climate Res*., Vol. 14, pp. 71-73.

Davies, H.C., 1976. A lateral boundary formulation for multi-level prediction models, *Quart. J. Roy. Meteor. Soc*., Vol. 102, pp. 405-418.

Feser, F., R. Weisse, and H. von Storch, 2001. Multi-decadal atmospheric modelling for Europe yields multi-purpose data, *EOS Transactions*, Vol. 82, pp. 305, 310.

Gaslikova, L. and R. Weisse, 2006. Estimating near-shore wave statistics from regional hindcasts using downscaling techniques. *Ocean Dynamics*, Vol. 56, pp. 26-35, doi:10.1007/s10236-005-0041-2.

Hervouet, J.M. and L. Van Haren, 1996. TELEMAC2D Version 3.0 Principle Note. Rapport EDF HE-4394052B, Electricité de France, Département Laboratoire National d'Hydraulique, Chatou CEDEX.

Jacob, D. and R. Podzun, 1997. Sensitivity studies with the regional climate model REMO, *Meteorol. Atmos. Phys*., Vol. 63, pp. 119-129.

Kalnay, E., M. Kanamitsu, R. Kistler, W. Collins, D. Deaven, L. Gandin, M. Iredell, S. Saha, G. White, J. Woollen, Y. Zhu, M. Chelliah, W. Ebisuzaki, W. Higgins, J. Janowiak, K.C. Mo, C. Ropelewski, J. Wang, A. Leetmaa, R. Reynolds, R. Jenne, and D. Joseph, 1996. The NCEP/NCAR reanalysis project, *Bull. Am. Meteorol. Soc*., Vol. 77, pp. 437-471.

Kistler, R., E. Kalnay, W. Collins, S. Saha, G. White, J. Wollen, M. Chelliah, W. Ebisuzaki, M. Kanamitsu, V. Kousky, H. van den Dool, R. Jenne, and M. Fioriono, 2001. The NCEP/NCAR 50-year reanalysis: Monthly means CD-ROM and documentation, *Bull. Am. Meteorol. Soc*., Vol. 82, pp. 247-267.

Koch, W. and F. Feser, 2006. Relationship between SAR derived wind vectors and wind at ten meters height represented by a mesoscale model, *Mon. Wea. Rev*., Vol. 134, pp. 1505-1517.

Plüß, A., 2004. Das Nordseemodell der BAW zur Simulation der Tide in der Deutschen Bucht, *Die Küste*, Vol. 67, pp. 83-127.

Soares, C.G., R. Weisse, J.C. Carretero, and E. Alvarez, 2002. A 40 years hindcast of wind, sea level and waves in European waters, *Proc. 21st International Conference on Offshore Mechanics and Arctic Engineering,* 23-28 June 2002, Norway, Oslo.

von Storch, H., H. Langenberg, and F. Feser, 2000. A spectral nudging technique for dynamical downscaling purposes, *Mon. Wea. Rev*., Vol. 128, pp. 3664-3673.

WAMDI-Group, 1988. The WAM model - a third generation ocean wave prediction model, *J. Phys. Oceanogr*., Vol. 18, pp. 1776-1810.

Weisse, R. and A. Plüß, 2006. Storm-related sea level variations along the North Sea coast as simulated by a high-resolution model 1958-2002, *Ocean Dynamics*, Vol. 56, pp. 16-25, doi:10.1007/s10236-005-0037-y.

Weisse, R. and H. Günther, 2006. Wave climate and long-term changes for the Southern North Sea obtained from a high-resolution hindcast 1958-2002, *Ocean Dynamics*, submitted.

Weisse, R., H. von Storch, and F. Feser, 2005. Northeast Atlantic and North Sea storminess as simulated by a regional climate model 1958-2001 and comparison with observations, *J. Climate*, Vol. 18, pp. 465-479, doi:10.1175/JCLI-3281.1.

Weisse, R. and F. Feser, 2003. Evaluation of a method to reduce uncertainty in wind hindcasts performed with regional atmosphere models, *Coastal Eng*., Vol. 48, pp. 211-225.